University of Milan

Faculty of Political, Economic and Social Sciences

A Bayesian Approach to Aggregate Insurance Claim Modeling

Final Project in the Subject Bayesian Analysis

Julia Maria Wdowinska (43288A)
Edoardo Zanone (33927A)

Data Science for Economics
II Year
Master's Degree

May 1, 2025

Contents

1 Introduction **1**

2 Theoretical Background **1**

3 Replication of Dudley (2006) **1**
3.1 Model Specification 2
3.2 Sampling Results 3
3.3 Convergence Diagnostics 3
3.4 Predictive Inference 6

4 Implementation on Alternative Data **9**

1 Introduction

2 Theoretical Background

In insurance modeling, accurately estimating the aggregate value of claims is essential for premium calculation, risk assessment, and maintaining solvency of insurance providers. The aggregate claim value refers to the total amount paid out for claims over a specified period. This quantity is typically modeled using a compound distribution, which separately describes the frequency and severity of claims. The frequency component, representing the number of claims within the period, is often modeled using a Poisson distribution. The severity component, which captures the magnitude of individual claims, is commonly modeled using heavy-tailed distributions such as the Pareto or Gamma distributions.

The traditional framework for modeling such processes is grounded in frequentist statistics. In this approach, the parameters of the underlying distributions—such as the Poisson rate parameter λ, or the shape and scale parameters α and β of the Pareto distribution—are considered fixed but unknown quantities. These parameters are typically estimated from observed data using techniques such as maximum likelihood estimation (MLE).

In contrast, the Bayesian framework treats these parameters as random variables characterized by prior distributions. This allows for the incorporation of prior knowledge or beliefs about the parameters before any data is observed. The prior distribution is updated using Bayes' theorem upon observing data, resulting in a posterior distribution that reflects the updated beliefs. This posterior distribution forms the basis for inference and prediction.

Bayesian methods offer significant advantages in insurance modeling. They are well-suited for incorporating expert knowledge or external information, handling limited or noisy datasets, and accommodating complex hierarchical structures commonly found in insurance data. Moreover, Bayesian inference provides a coherent framework for uncertainty quantification by yielding full posterior distributions over model parameters.

Nevertheless, Bayesian methods also come with certain limitations. The choice of prior distribution can introduce subjectivity, and computational complexity can be significant, especially in models with high dimensionality or non-conjugate priors. Despite these challenges, the flexibility and robustness of the Bayesian framework make it a valuable approach for modeling aggregate insurance claims.

3 Replication of Dudley (2006)

Building on the theoretical background, this project aims to replicate the Bayesian modeling approach proposed by Dudley (2006). The analysis is based on a dataset of automobile insurance claims exceeding 1.5 million, collected over a five-year period. The data, originally reported by Rytgaard (1990), is presented in Table 1.

Table 1: Insurance Claim Amounts Exceeding 1.5 Million (Data from Rytgaard, 1990)

Year	**Claim Amounts (in millions)**				
1	2.495	2.120	2.095	1.700	1.650
2	1.985	1.810	1.625	–	–
3	3.215	2.105	1.765	1.715	–
4	–	–	–	–	–
5	19.180	1.915	1.790	1.755	–

The threshold of 1.5 million corresponds to the retention level of an excess-of-loss insurance policy[1].

[1]To manage risk exposure, insurers frequently employ reinsurance strategies, which help reduce their financial liability on large claims. Under such arrangements, if a claim amount y exceeds a predetermined threshold d (the retention), the insurer is responsible

3.1 Model Specification

To model this dataset within a Bayesian framework, assumptions about the distributions of both the number of claims in year t (N_t) and the amount of the i-th claim in year t ($Y_{i,t}$) were necessary. Claims were assumed to occur randomly and independently at a constant rate over time, so N_t was modeled using a Poisson distribution. A Pareto distribution was selected for $Y_{i,t}$, as a heavy-tailed loss distribution was needed to account for the fact that individual claim amounts are positive and may include large outliers. That is,

$$\begin{aligned} N_t &\sim \text{Poisson}(\theta), \quad 0 < \theta < \infty, \\ Y_{i,t} &\sim \text{Pareto}(\alpha, \beta), \quad \alpha > 0, \quad 0 < \beta < y. \end{aligned}$$

The Pareto(α, β) distribution with support $[\beta, \infty)$ was particularly suitable in this context, as it was employed to model claim amounts exceeding a specified threshold.

In addition, the following assumptions were made:

- N_t are independently and identically distributed (i.i.d.) across t,
- $Y_{i,t}$ are i.i.d. across both i and t,
- N_t and $Y_{i,t}$ are independent for all i and t.

Under these assumptions, the aggregate claim amount in year t was defined as

$$S_t = Y_{1,t} + Y_{2,t} + \cdots + Y_{N_t,t}.$$

Next, prior distributions for the parameters α, β, and θ were specified. Due to limited prior knowledge about their true values—beyond the assumption that they are strictly positive—vague Gamma priors[2] were chosen:

$$\alpha \sim \text{Gamma}(1, 0.0001), \quad \beta \sim \text{Gamma}(1, 0.0001), \quad \theta \sim \text{Gamma}(1, 0.0001),$$

with the constraint $0 < \beta < \min\{y_{i,t}\}$ to ensure validity of the Pareto distribution.

Finally, the posterior distributions were derived. First, the joint posterior distribution of (α, β) was obtained via Bayes' theorem[3]:

$$\begin{aligned} \pi(\alpha, \beta \mid \mathbf{y}) &\propto \pi(\alpha) \cdot \pi(\beta) \cdot f(\mathbf{y} \mid \alpha, \beta) \\ &\propto 0.0001 \cdot \exp(-0.0001\alpha) \cdot 0.0001 \cdot \exp(-0.0001\beta) \cdot \prod_{i=1}^{n} \frac{\alpha \beta^{\alpha}}{y_i^{\alpha+1}} \\ &\propto \exp(-0.0001\alpha) \cdot \exp(-0.0001\beta) \cdot \alpha^n \cdot \beta^{n\alpha} \left(\prod_{i=1}^{n} y_i \right)^{-(\alpha+1)} \\ &\propto \alpha^n \cdot \exp(-0.0001\alpha) \cdot \left(\prod_{i=1}^{n} y_i \right)^{-\alpha} \cdot \beta^{n\alpha} \cdot \exp(-0.0001\beta) \\ &\propto \alpha^n \cdot \exp\left(- \left(0.0001 + \sum_{i=1}^{n} \ln(y_i) \right) \alpha \right) \cdot \beta^{n\alpha} \cdot \exp(-0.0001\beta) \end{aligned}$$

As a result, the full conditional posterior distributions of α and β were as follows:

$$\begin{aligned} \pi(\alpha \mid \beta, \mathbf{y}) &\propto \alpha^n \cdot \exp\left(- \left(0.0001 - n \ln(\beta) + \sum_{i=1}^{n} \ln(y_i) \right) \alpha \right), \\ \pi(\beta \mid \alpha, \mathbf{y}) &\propto \beta^{n\alpha} \cdot \exp(-0.0001\beta), \end{aligned}$$

which implied that:

$$\begin{aligned} \alpha \mid \beta, \mathbf{y} &\sim \text{Gamma}\left(n + 1, \sum_{i=1}^{n} \ln(y_i) - n \ln(\beta) + 0.0001 \right), \\ \beta \mid \alpha, \mathbf{y} &\sim \text{Gamma}(n\alpha + 1, 0.0001). \end{aligned}$$

only for paying up to d, while any excess $y - d$ is covered by the reinsurer.

[2]Each of these Gamma priors has a variance of 10^8, implying minimal prior influence so that most of the information about the parameters is derived from the dataset. Additionally, the Gamma distribution is conjugate to both the Poisson and Pareto likelihoods, facilitating analytical tractability in Bayesian inference.

[3]Here, assuming that α and β are independent, the joint prior $\pi(\alpha, \beta)$ was computed as $\pi(\alpha) \cdot \pi(\beta)$.

Similarly, the posterior distribution of θ was obtained via Bayes' theorem:

$$\begin{aligned}\pi(\theta \mid \mathbf{n}) &\propto \pi(\theta) \cdot f(\mathbf{n} \mid \theta) \\ &\propto \exp(-0.0001\theta) \cdot \prod_{t=1}^{T} (\theta^{n_t} \cdot \exp(-\theta)) \\ &\propto \exp(-0.0001\theta) \cdot \theta^{\sum_{t=1}^{T} n_t} \cdot \exp(-5\theta) \\ &\propto \exp(-5.0001\theta) \cdot \theta^{\sum_{t=1}^{T} n_t}\end{aligned}$$

which implied that:

$$\theta \mid \mathbf{n} \sim \text{Gamma}\left(\sum_{t=1}^{T} n_t + 1, 5.0001\right)$$

3.2 Sampling Results

Since all three posterior distributions were standard distributions, the Gibbs sampling method was employed to draw realizations from them[4]. This was implemented using the `JAGS` program, which was called from within `R`. Following Dudley (2006), three Markov chains were run in parallel. The initial values of α, β, and θ were chosen to be well-dispersed and are presented in Table 2.

Table 2: Initial Parameter Values

Chain	α	β	θ
1	0.000 01	0.000 01	0.000 01
2	100 000	1	100 000
3	3.076	1.625	3.200

These values are taken from Dudley (2006).

A burn-in of 20,000 iterations was used. The statistics computed from the subsequent 30,000 iterations are presented in Table 11. A comparison with those reported by Dudley (2006) shows a close match, indicating that the model was properly specified and the Gibbs sampler executed correctly.

Table 3: Posterior Statistics

	Mean	**Standard Deviation**	**95% Bayesian Credible Interval**
α	3.076	0.762	(1.762, 4.752)
β	1.591	0.035	(1.498, 1.624)
θ	3.399	0.820	(1.986, 5.185)
$E[Y]$	2.507	1.071	(2.024, 3.637)

$E[Y]$ was calculated for each simulated set of parameters α and β, and from these values, the mean, standard deviation, and 95% Bayesian credible interval were subsequently computed.

In addition, density plots were generated for each of the parameters and for $E[Y]$, as presented in Figure 1. The resulting densities for the parameters resemble Gamma distributions, with the density of β appropriately truncated at $\min\{y_{i,t}\} = 1.625$. The plot for $E[Y]$ displays a right-skewed distribution that permits very large values, albeit with very low probability—consistent with expectations.

The posterior means of α and β were used as parameters of the Pareto distribution, and the corresponding cumulative distribution function (CDF) was plotted against the empirical cumulative data ($y_{i,t}$). Similarly, the posterior mean of θ was used as the parameter of the Poisson distribution, and its CDF was plotted against the empirical cumulative data (n_t). The Pareto(3.079, 1.592) distribution provides a close fit to the empirical data. The Poisson(3.396) distribution also fits the observed frequencies quite well (see Figures 2 and 3).

3.3 Convergence Diagnostics

Throughout all computations above, it was assumed that the Markov chains had converged to a stationary distribution after discarding the initial 20,000 iterations, following the approach of Dudley (2006). However, it was essential to verify that convergence had indeed occurred. The first method of assessment involved visual inspec-

[4]Markov Chain Monte Carlo (MCMC) methods, like Gibbs sampling, are used to draw samples from intractable posterior distributions. Gibbs sampling is efficient when full conditional posteriors are in closed form, often with conjugate priors. When posteriors are not in closed form, the Metropolis-Hastings algorithm can be used to generate candidate values from a proposal distribution.

Figure 1: Posterior Densities

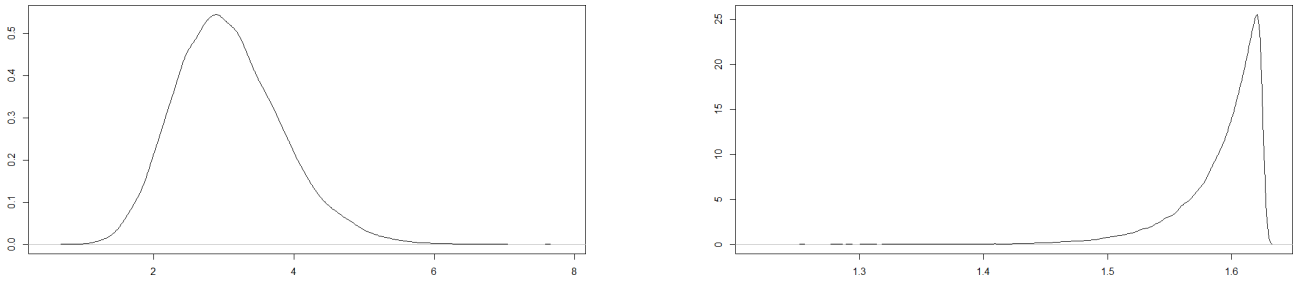

(a) α

(b) β

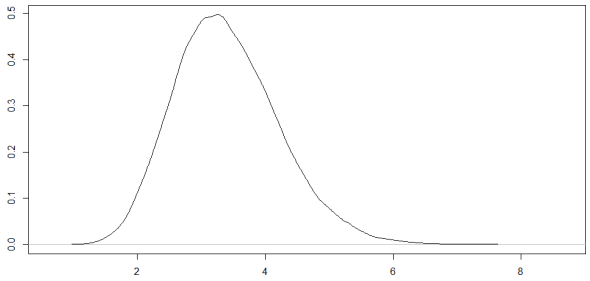

(c) θ

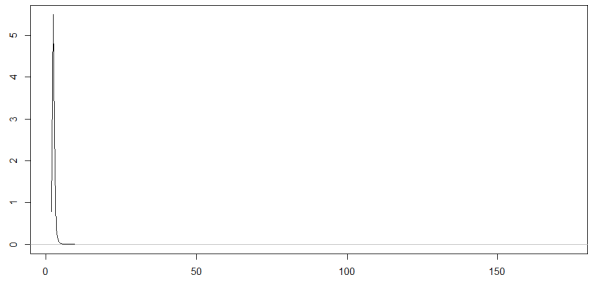

(d) $E[y]$

Figure 2: Empirical vs. Fitted Pareto CDF

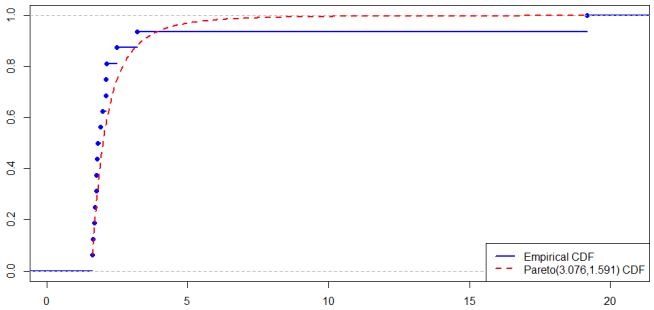

Figure 3: Empirical vs. Fitted Poisson CDF

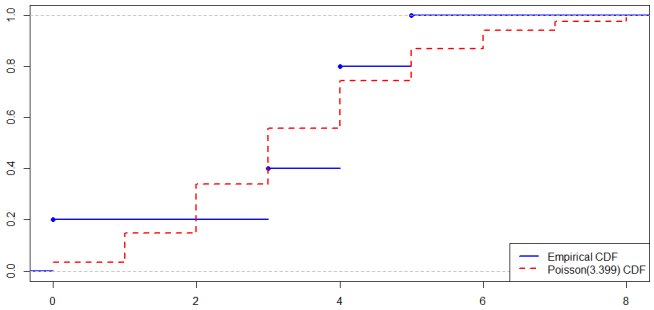

tion[5]. Figure 4 presents trace plots for all three parameters, showing the sampled values across iterations. These plots indicate good mixing, suggesting that the chains have likely converged.

Convergence was further assessed using the Gelman–Rubin diagnostic (Gelman and Rubin, 1992), applied to the post-burn-in iterations (20,001–50,000). The results, shown in Table 4, indicate that all univariate potential scale reduction factors (PSRFs) have point estimates and upper confidence bounds equal to 1. The multivariate PSRF is also 1. These values again suggest that the Markov chains have likely converged, both individually and jointly.

Figure 5 shows how the univariate PSRF point estimates evolve with increasing iterations. Throughout all iterations, all estimates remain below 1.1, which is commonly considered an acceptable threshold for convergence.

[5]Visual inspection involves assessing how well a chain explores the parameter space. Poor mixing—where the chain moves slowly or gets stuck—indicates potential convergence issues. Trace plots help identify such problems by showing how sampled values evolve over iterations for each parameter.

Figure 4: Trace Plots

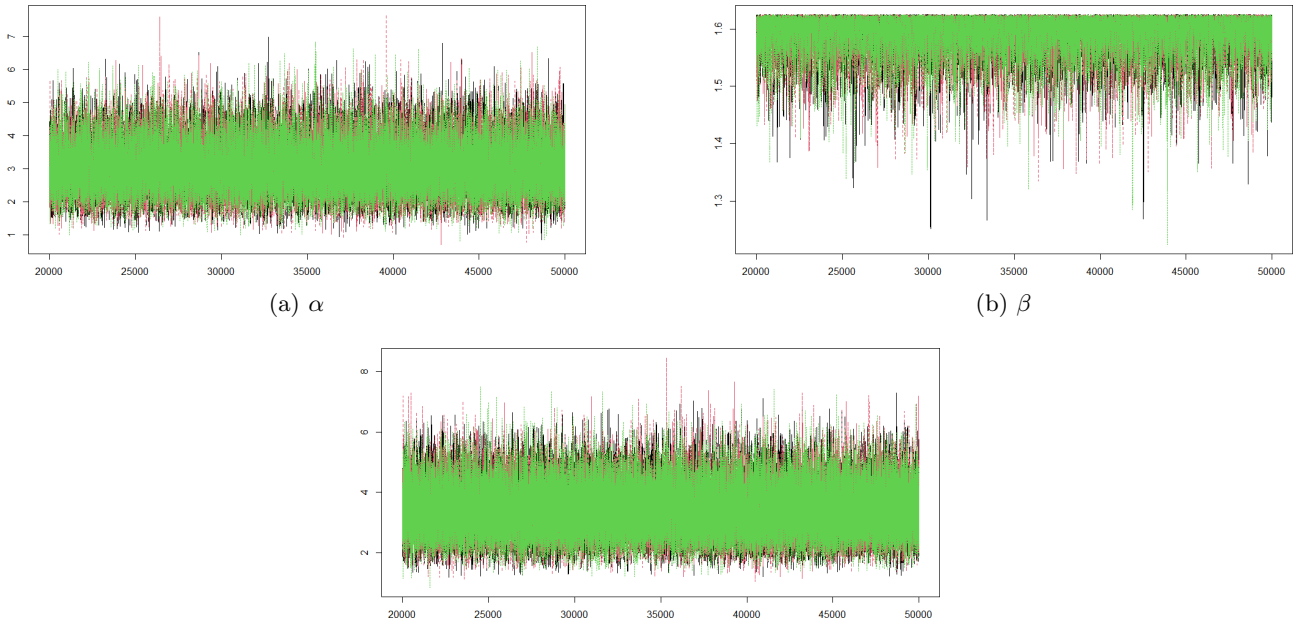

(a) α (b) β

(c) θ

Table 4: Potential Scale Reduction Factors (Gelman–Rubin Diagnostic)

Parameter	Point Estimate	Upper C.I.
α	1.00	1.00
β	1.00	1.00
θ	1.00	1.00
Multivariate PSRF	1.00	

The diagnostic was applied to iterations 20,001–50,000.

This further confirms that the chains have likely reached a stable distribution.

Figure 5: PSRF Values (Gelman–Rubin Diagnostic)

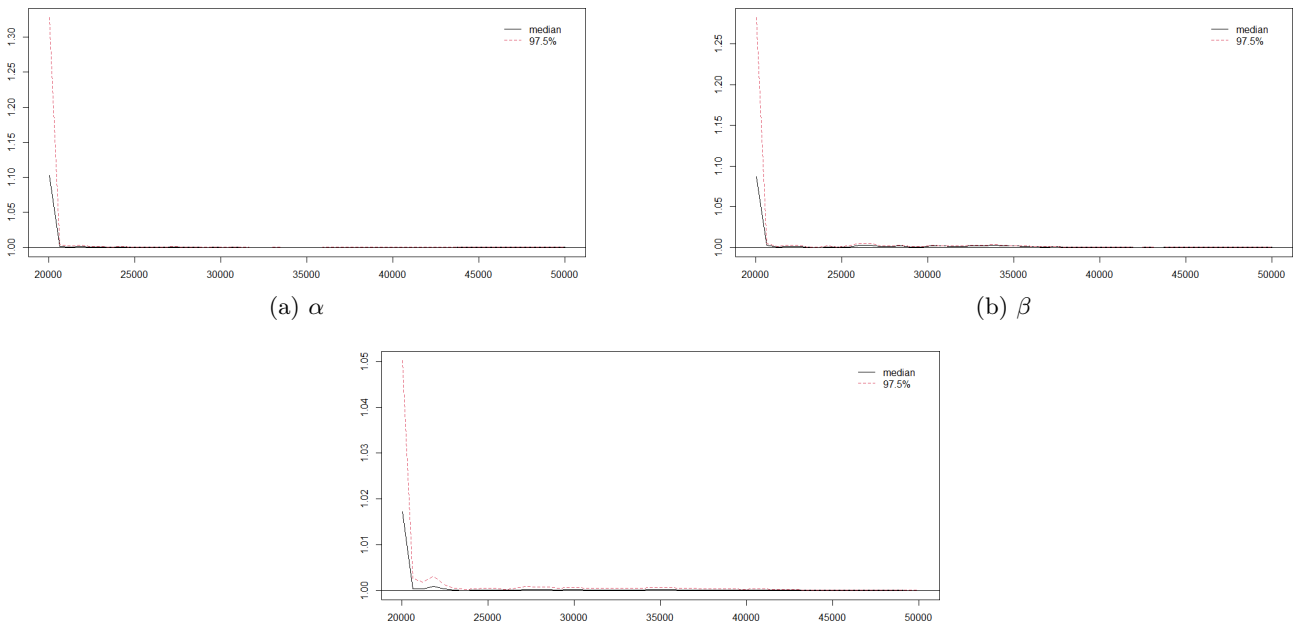

(a) α (b) β

(c) θ

In addition, autocorrelation[6] plots were generated for all three parameters (see Figure 6), and values at lags

[6]The autocorrelation function (ACF) shows the correlation between samples at different lags. High autocorrelation indicates strong dependence between draws, leading to slow mixing. Thinning reduces this dependence by keeping only every kth sample.

1 through 10 are reported in Table 5. Several high autocorrelations were observed, particularly for β, which motivated the use of a thinning interval of 10 iterations, as suggested by Dudley (2006).

Figure 6: Autocorrelation Plots

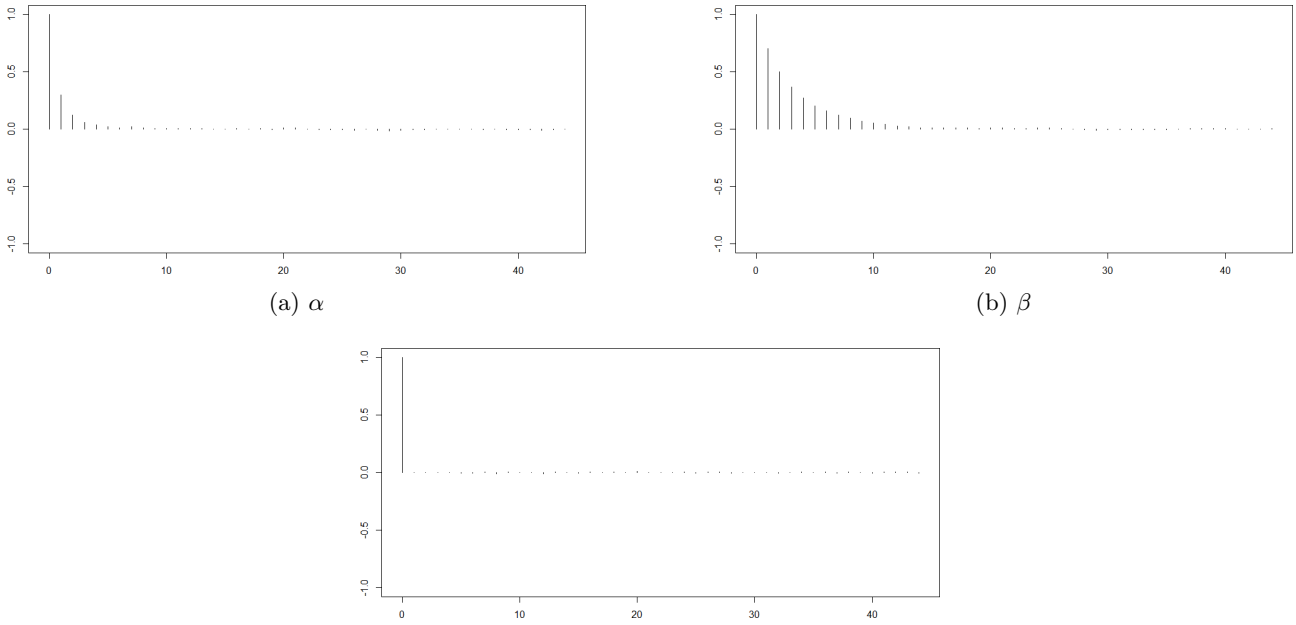

(a) α

(b) β

(c) θ

Table 5: Autocorrelations at Lags 1–10

Lag	α	β	θ
1	0.288	0.699	−0.001
2	0.109	0.498	−0.001
3	0.053	0.356	0.003
4	0.035	0.257	−0.007
5	0.019	0.191	0.002
6	0.008	0.144	−0.006
7	0.010	0.104	0.003
8	0.013	0.079	−0.007
9	0.007	0.061	0.001
10	0.006	0.048	0.000

Consequently, the chains were rerun with this thinning. Figure 7 presents the corresponding trace plots, and Figure 8 shows the updated autocorrelation plots. The trace plots indicate that the chains have mixed well, and the autocorrelation plots demonstrate that all autocorrelation values at lags 1, 2, and beyond have become negligible.

3.4 Predictive Inference

The ultimate objective of the analysis was to predict future values of S_t, which was accomplished using the posterior predictive distribution. For a variable z, this distribution is defined as[7]:

$$\pi(z \mid \mathbf{y}) = \int_{\Theta} f(z \mid \phi)\, \pi(\phi \mid \mathbf{y})\, d\phi$$

where $\pi(\phi \mid \mathbf{y})$ is the posterior distribution of ϕ, and $f(z \mid \phi)$ is the likelihood of z given ϕ.

Let $\mathbf{n}$ denote the observed data, and let N_f represent a future observation of N_t. Then the posterior predictive distribution of N_f is given by:

$$\begin{aligned} p(N_f = n \mid \mathbf{n}) &= \int_0^{\infty} p(N_f = n \mid \theta)\pi(\theta \mid \mathbf{n})\, d\theta \\ &= \mathbb{E}_{\theta|\mathbf{n}}\left[p(N_f = n \mid \theta)\right] \\ &= \mathbb{E}_{\theta|\mathbf{n}}\left[\frac{\theta^n e^{-\theta}}{n!}\right] \end{aligned}$$

[7]This method accounts for the uncertainty in $\boldsymbol{\phi}$ by integrating over its possible values, weighted by their posterior probabilities.

Figure 7: Trace Plots After Thinning

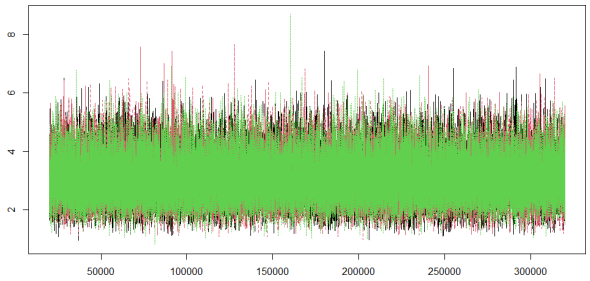

(a) α

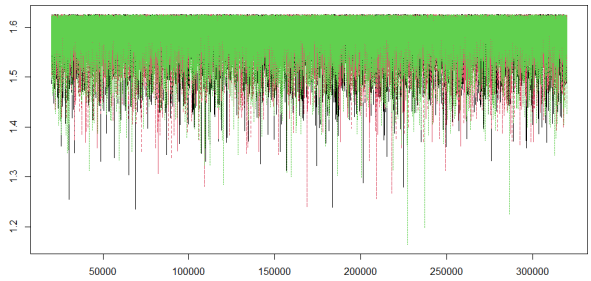

(b) β

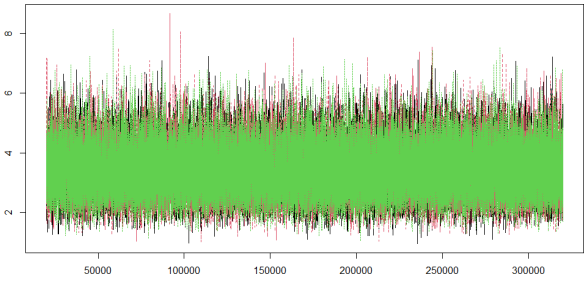

(c) θ

Figure 8: Autocorrelation Plots After Thinning

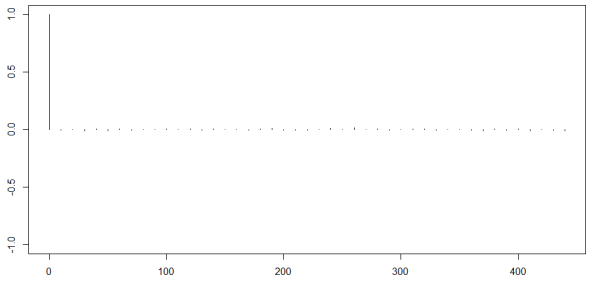

(a) α

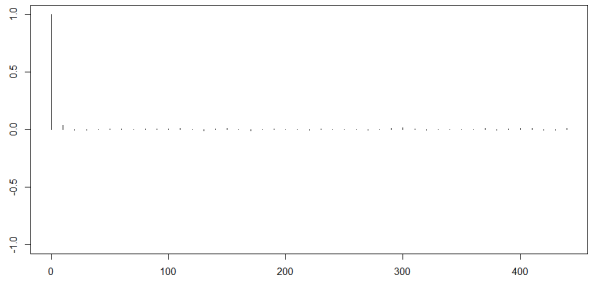

(b) β

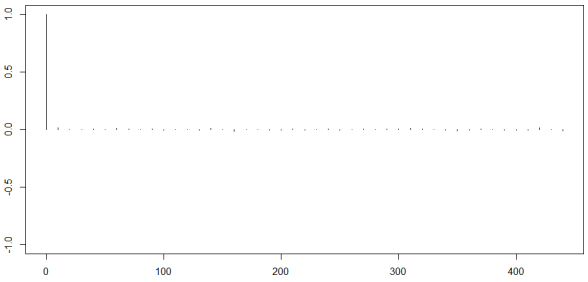

(c) θ

Since the integral cannot be evaluated analytically, it is typically approximated using samples from the posterior distribution obtained via MCMC. Specifically, the expectation is approximated as:

$$p(N_f = n \mid \mathbf{n}) \approx \frac{1}{m} \sum_{i=1}^{m} \frac{(\theta^{(i)})^n e^{-\theta^{(i)}}}{n!}$$

where $\theta^{(i)}$ is the i-th sample from the MCMC chain and m is the number of iterations after burn-in and thinning.

Similarly, let $\mathbf{y}$ denote the observed data, and let Y_f represent a future observation of $Y_{i,t}$. Then the posterior predictive cumulative distribution function (CDF) of Y_f is given by:

$$\begin{aligned} p(Y_f \leq y \mid \mathbf{y}) &= \int_{\mathbf{u}} p(Y_f \leq y \mid \mathbf{u})\, \pi(\mathbf{u} \mid \mathbf{y})\, d\mathbf{u} \\ &= \mathbb{E}_{\mathbf{u}|\mathbf{y}} \left[p(Y_f \leq y \mid \alpha, \beta) \right] \end{aligned}$$

Again,

$$p(Y_f \leq y \mid \mathbf{y}) \approx \frac{1}{m} \sum_{i=1}^{m} \left(1 - \left(\frac{\beta^{(i)}}{y} \right)^{\alpha^{(i)}} \right)$$

where $\alpha^{(i)}$ and $\beta^{(i)}$ denote the i-th samples from the MCMC chain.

Table 6 shows the estimated probabilities of $N_f = n$ for $n = 0, \ldots, 14$, which are consistent with the findings of Dudley (2006). Figure 9 displays the estimated predictive probability density function (PDF) of Y_f, obtained using the inverse CDF method[8].

Table 6: Estimates of $p(N_f = n \mid \mathbf{n})$

n	**Probability**
0	0.0453
1	0.1282
2	0.1919
3	0.2023
4	0.1683
5	0.1177
6	0.0718
7	0.0393
8	0.0196
9	0.0091
10	0.0039
11	0.0016
12	0.0006
13	0.0002
14	0.0001

Figure 9: Estimated Predictive PDF of Y_f

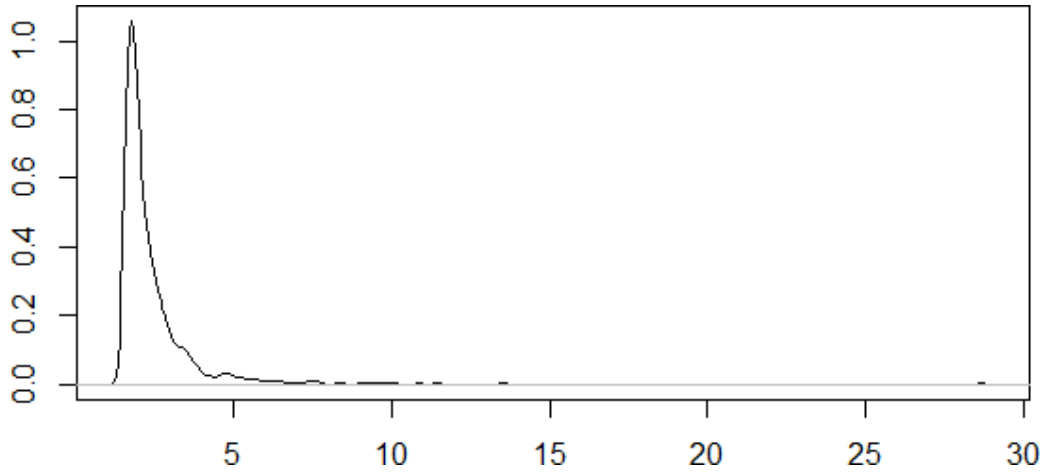

The draws of S_f, representing a future observation of S_t, were generated as follows:

1. 1,000 values of N_f were drawn using the inverse CDF method[9].
2. For each simulated value of N_f, the corresponding number of Y_f values was drawn using the same procedure as in the predictive PDF estimation, and these values were then summed to generate a draw of S_f.

Figure 10 presents the histogram of the resulting S_f samples, along with three fitted distributions using moment matching. As observed by Dudley (2006), the Gamma distribution provides the best fit. The fitted Gamma distribution has parameters $\alpha = 1.726$ and $\beta = 0.202$.

Table 7 reports various percentiles of the simulated S_f values. The maximum value of 116.396 reflects a long tail, consistent with expectations for a heavy-tailed claim size distribution. This indicates that the simulation effectively captured the tail behavior of the predictive distribution of S, which is important since most aggregate claims are moderate, but extreme values can occasionally occur.

[8]Specifically, 1,000 values $U \sim \text{Uniform}(0, 1)$ were generated. For each value, the transformation $\beta^{(i)}(1-U)^{-1/\alpha^{(i)}}$ was applied for each i, and the results were averaged across i. The resulting 1,000 values were then used to approximate the PDF of Y_f via kernel density estimation (KDE).

[9]Once again, 1,000 values $U \sim \text{Uniform}(0, 1)$ were generated. For each value, Poisson samples were drawn for each $\theta^{(i)}$ using the inverse CDF method. The results were averaged across i and rounded to produce 1,000 integer values.

Figure 10: Histogram and Fitted Distributions for Predictive S_f

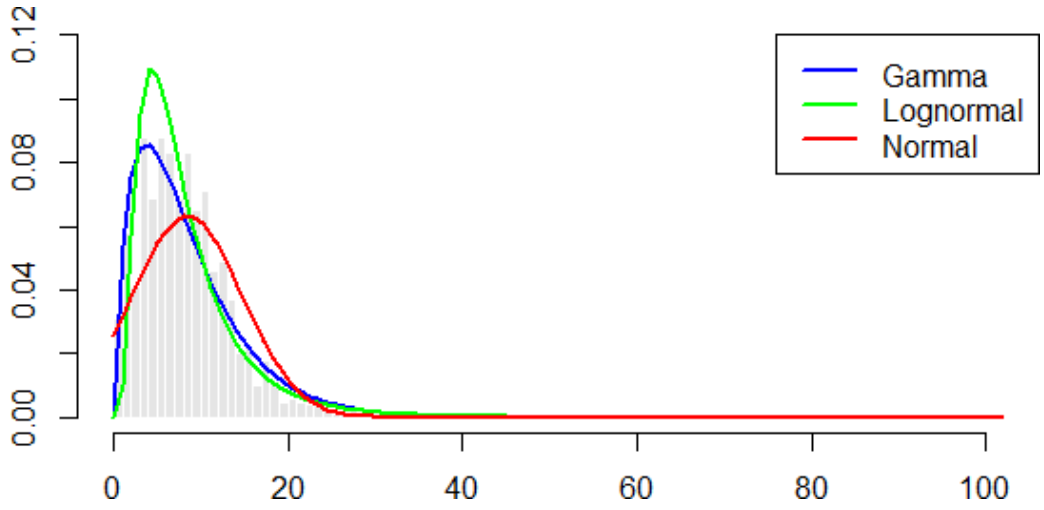

Table 7: Percentiles of Simulated S_f Values

Percentile	Value
Median	7.504
90th Percentile	15.065
95th Percentile	18.092
99th Percentile	25.171
Maximum	116.396

4 Implementation on Alternative Data

To evaluate the generalizability of Dudley (2006) Bayesian approach to insurance claim modeling, the same methodology was applied to an alternative dataset. The `itamtplcost` dataset contains 457 individual motor insurance claims exceeding 500,000 euros, recorded in Italy between 1997 and 2012 (Dutang, 2020).

Table 8 reports a comparison of summary statistics between the Rytgaard (1990) and `itamtplcost` datasets. It is evident that claims in the `itamtplcost` dataset are significantly larger, with a mean of 1,015.352 million euros compared to 3.058 million euros in the Rytgaard (1990) dataset. The variability is also higher, with a range of 6,637.339 compared to 17.555. These differences render the dataset more complex and provide a valuable test of whether the Gamma–Pareto–Poisson model continues to yield meaningful posterior inference and predictions in a more realistic insurance context.

Table 8: Comparison of Summary Statistics Between Datasets

Dataset	Min	1st Qu.	Median	Mean	3rd Qu.	Max
			Claim Amounts (in millions)			
Rytgaard (1990)	1.625	1.745	1.863	3.058	2.109	19.180
`itamtplcost`	2.161	627.719	844.011	1015.352	1224.316	6639.500
			Claim Counts			
Rytgaard (1990)	0.00	3.00	4.00	3.20	4.00	5.00
`itamtplcost`	5.00	24.25	30.50	28.56	35.25	40.00

Similarly to the previous case, Gibbs sampling was used to draw realizations from the posterior distributions of α, β, and θ. Three Markov chains were run in parallel, with initial parameter values chosen to be well-dispersed (see Table 9). For the third chain, the initial values were set to the maximum likelihood estimates (MLEs) of the parameters.

Table 9: Initial Parameter Values (`itamtplcost`)

Chain	α	β	θ
1	0.000 01	0.000 01	0.000 01
2	100 000	1.330	100 000
3	0.169	2.161	28.563

Initially, a burn-in of 5,000 iterations was employed, and the Gelman–Rubin diagnostic (Gelman and Rubin, 1992) was used to assess if this was sufficient. Figure 11 shows how the univariate PSRF point estimates evolve with the number of iterations. While all estimates remain below 1.1, they stabilize around 1 at approximately the

10,000th iteration. Therefore, a burn-in of 10,000 was adopted. The chains were rerun, and autocorrelation plots were then generated (see Figure 12), with values at lags 1 through 10 reported in Table 10. High autocorrelations were observed, particularly for β, and thus a thinning interval of 10 was applied.

Figure 11: PSRF Values (Gelman–Rubin Diagnostic) (`itamtplcost`)

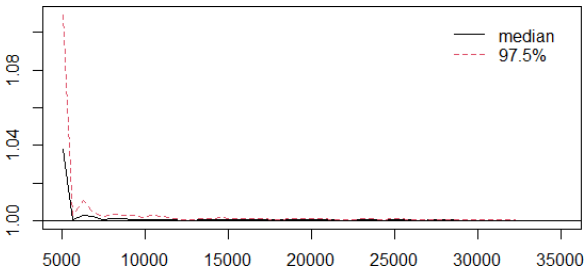

(a) α

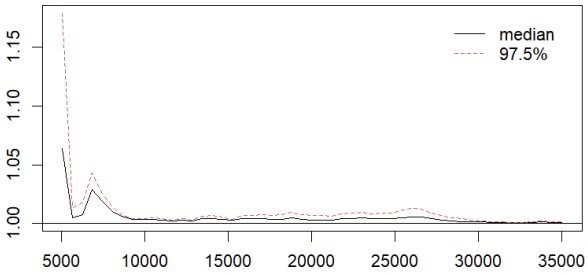

(b) β

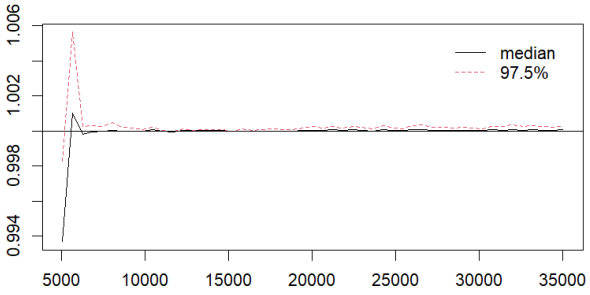

(c) θ

Figure 12: Autocorrelation Plots (`itamtplcost`)

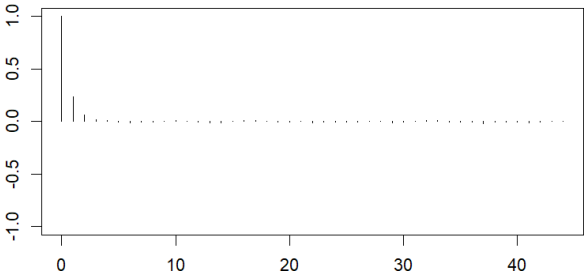

(a) α

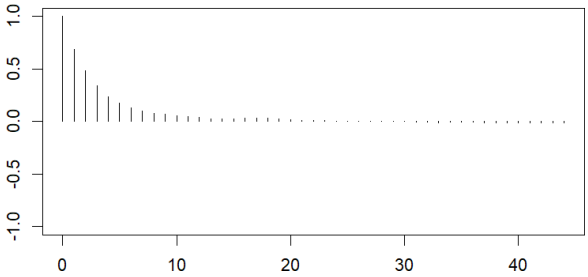

(b) β

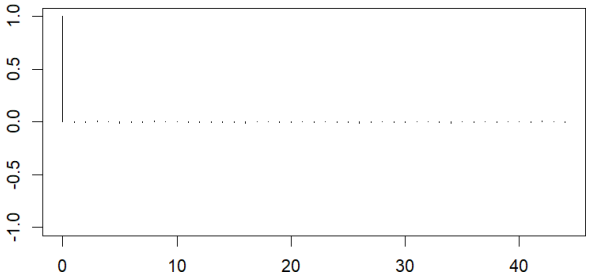

(c) θ

The chains were rerun with this thinning. Figure 13 presents the trace plots, while Figure 14 shows the updated autocorrelation plots. The trace plots indicate good mixing across chains, and the autocorrelation plots demonstrate that autocorrelation values at all lags have become negligible.

Table **??** reports statistics computed from 30,000 post-burn-in iterations, while Figure **??** presents the posterior density plots for α, β, and θ. The resulting densities resemble Gamma distributions, with the density of β appropriately truncated at 0.002, reflecting the minimum value of y. The statistics and density plot for $E[y]$ could not be obtained for the `itamtplcost` dataset, as all posterior draws of α were below 1—implying that the expected value of the Pareto distribution is undefined in this case.

Table 10: Autocorrelations at Lags 1–10 (`itamtplcost`)

Lag	α	β	θ
1	0.146	0.679	−0.003
2	0.032	0.472	−0.006
3	0.011	0.327	−0.002
4	0.009	0.228	0.002
5	0.001	0.166	−0.003
6	−0.005	0.121	−0.004
7	−0.003	0.085	0.004
8	0.000	0.061	0.004
9	0.000	0.046	−0.004
10	−0.001	0.032	−0.001

Figure 13: Trace Plots After Thinning (`itamtplcost`)

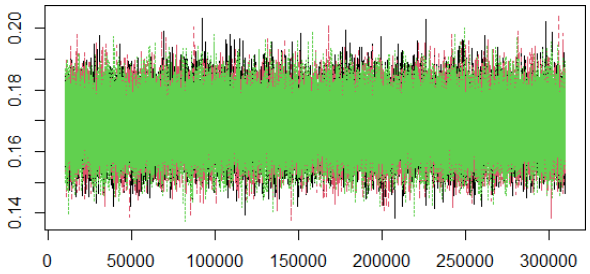

(a) α

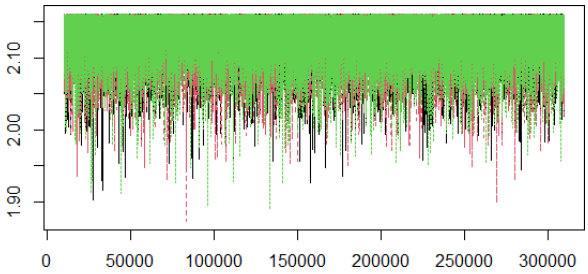

(b) β

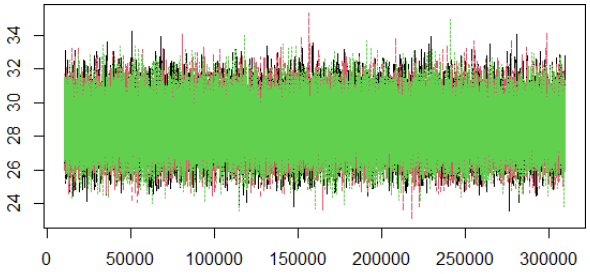

(c) θ

Figure 14: Autocorrelation Plots After Thinning (`itamtplcost`)

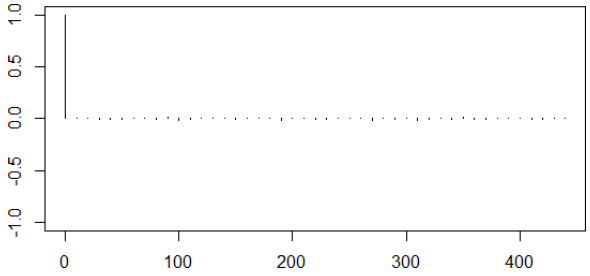

(a) α

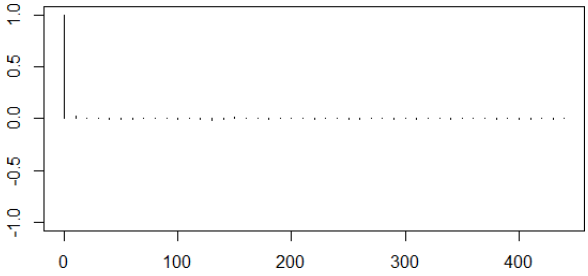

(b) β

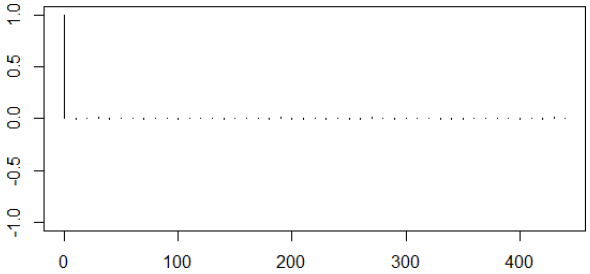

(c) θ

References

Dudley, C. (2006). Bayesian Analysis of an Aggregate Claim Model Using Various Loss Distributions. Master's dissertation, Heriot-Watt University, School of Mathematical and Computer Sciences, Actuarial Mathematics

Table 11: Posterior Statistics (`itamtplcost`)

	Mean	**Standard Deviation**	**95% Bayesian Credible Interval**
α	3.076	0.762	(1.762, 4.752)
β	1.591	0.035	(1.498, 1.624)
θ	3.399	0.820	(1.986, 5.185)

& Statistics.

Dutang, C. (2020). CASdatasets: Insurance Datasets. R package version 1.0.

Gelman, A. and Rubin, D. B. (1992). Inference from Iterative Simulation Using Multiple Sequences. *Statistical Science*, 7(4):457–472.

Rytgaard, M. (1990). Estimation in the Pareto Distribution. *ASTIN Bulletin*, 20(2):201–216.